# Looking beyond the active substance: Comprehensive dissipation study of myclobutanil-based plant protection product in tomato and grape using chromatographic techniques coupled to high resolution mass spectrometry

Jesús Marín-Sáez,[a*] Rosalía López-Ruiz,[a] Roberto Romero-Gonzalez,[a] Antonia Garrido Frenich,[a] Ismael Zamora Rico[b]

[a]Department of Chemistry and Physics, Analytical Chemistry Area, University of Almería Research Centre for Agricultural Food Biotechnology (BITAL), Agrifood Campus of International Excellence ceiA3, Carretera de Sacramento s/n, E-04120 Almería, Spain

[b]Lead Molecular Design, SL Valle's, Barcelona, Spain

**ORCID CODES**

Jesús Marín-Sáez: 0000-0002-4153-9788

Rosalía López-Ruiz: 0000-0003-0806-9013

Roberto Romero-González: 0000-0002-2505-2056

Antonia Garrido Frenich: 0000-0002-7904-7842

* Corresponding author at: University of Almería, Carretera de Sacramento s/n, E, 04120 Almería, Spain. E-mail address: jms485@ual.es (Jesús Marín Sáez).

**Abstract**

A comprehensive evaluation of the dissipation of a myclobutanil plant protection product (PPP) was performed in tomato and grape samples. Different temperature conditions (3 and 22°C) were evaluated. Biphasic kinetic model provided a suitable adjustment ($R^2$>0.95), with persistence (Residual level, $RL_{50}$) lower than 24 days in all cases. Solid-liquid extraction (SLE) and ultra-high performance liquid chromatography coupled to high resolution mass spectrometry (UHPLC-Q-Orbitrap-HRMS) were used for metabolites' elucidation, identifying six myclobutanil metabolites, four out of them described for the first time and one of them confirmed using $^{1}H$, $^{13}C$, ($^{1}H$-$^{1}H$)-COSY, ($^{1}H$-$^{13}C$)-HMQC and ($^{1}H$-$^{13}C$)-HMBC nuclear magnetic resonance (NMR). Their degradation curves were also evaluated, increasing their concentrations when myclobutanil concentration decreases. Additionally, co-formulants present in the commercial formulation were monitored employing headspace solid-phase microextraction method (HS-SPME)-gas chromatography coupled to HRMS (GC-Q-Orbitrap-HRMS). Seven co-formulants were quantified in tomato samples. Their dissipation curves were studied, observing they were almost degraded 12 days after application.

**Keywords**

Myclobutanil, dissipation, metabolites, HRMS, co-formulants, NMR

## Introduction

Pesticides are compounds worldwide used to treat any pest and they can be classified as herbicides, insecticides, fungicides, acaricides, rodenticides, etc.[1] To avoid pests and increase productivity they are y used in crops as tomato and grape, which are some of the crops where more active principles are used.[2] However, they can also cause several health problems as headaches, nausea, cancer, genetic diseases, etc, as well as the contamination of soil, air and water.[3] Tomato and grape cultivations are important in countries as Spain, being the eighth country producer of tomato, and the fourth of grape.[4] Besides, tomato is considered a high-water matrix while grape is considered a high sugar content matrix, so the behaviour of pesticides could be different. One of the most important pests for these cultivations is the fungus pest since cultivation is made at high temperatures and humidity. To control fungus pests, triazole fungicides, compounds containing 1,2,4-triazole groups in their structure, are widely employed.[5] Regarding this issue, myclobutanil is used for the control of powdery mildew and scabbing of plants and it acts by the inhibition of the ergosterol biosynthesis, a critical component of fungal cell membranes. Although myclobutanil and its dissipation have been extensively studied, even at different temperatures,[6] only a few metabolites have been elucidated and considering metabolites could be as toxic as parent compounds, this is an important issue. In bibliography, several metabolites as RH-9090, RH-9089 (produced by plant metabolism), RH-0294 (stable in milk), RH-8812, RH-8813 and butyric acid (soil metabolite), in addition to common triazole metabolites as free triazole, 1,2,4-triazole (T), and its 2 conjugates, triazolylalanine (TA) and triazolylacetic acid (TAA) (**Table 1**) were described.[7–9] It has to be clarified that the metabolites/impurities RH-8812 and RH-8813 are mentioned in EFSA document,[9] but information about them was not found, including formula or structure, so it cannot be included in conventional databases. The study of both known and unknown metabolites is an important issue since, for example, for known metabolites there is not toxicity data, and EFSA suggested that they have the same range of toxicity than the parent compound.[9]

Besides, together with the active substances there are other compounds added to the plant protection products (PPPs) which are not normally analysed. These compounds could be classified by the European Union (EU) Regulation 1107/2009,[10] as: protectors, added to reduce the toxic effects of the active substances; synergistic, which increases the action of the active substance; co-formulants, that are not protectors or synergistic; adjuvants, to improve the efficacy of the active substance application. In the case of co-formulants, they have an important economic impact with a market share expected to increase up to $4.400 million in 2026.[11] Despite of the beneficial characteristics provided by these compounds, they can cause health and environmental problems if they are consumed, as the narcotic and toxic effect of naphtha derivatives contained in the PPPs.[12] However, their presence and/or dissipation have been barely studied in foodstuffs or environmental samples.[13]

Legislation about PPPs is scarce and only the Regulation EC No 2021/383[14] includes the co-formulants unacceptable for inclusion in PPPs, while for myclobutanil as for other active substances there is a strict legislation. For example, in the EU, the European Commission establishes maximum residue limits (MRLs) for pesticides, and for myclobutanil this value is set at 1.5 and 0.6 mg/kg for grape and tomato respectively.[15]

The extraction of these compounds is affected by their physiochemical properties. Thus, myclobutanil is consider a compound with medium polarity, $K_{wo}$ of 776 (considering nonpolar compounds those with $K_{wo}$ higher than 1000, and polar those with lower $K_{wo}$). The most used technique to extract this compound is QuEChERS method (quick, easy, cheap, effective, rugged, and safe) or solid-liquid extraction (SLE), employing methanol or acetonitrile as extractant solvents.[8,16] However, QuEChERS approach does not allow for the extraction of polar compounds and considering that metabolites are normally more polar than parent compounds, SLE method could be more appropriated for this purpose. In general, co-formulants are analysed directly by dilution of the PPP and injection in the chromatographic system. A few studies evaluated the presence of surfactants in the aqueous environment applying liquid-liquid extraction (LLE),[17] in

marine sediments employing ultrasonic assisted extraction (USAE),[18] and in aquatic systems by USAE and solid-phase extraction (SPE).[19] Up to know, only one article published in 2021 evaluates the co-formulant dissipation in treated samples using a QuEChERS AOAC method, although it only includes the most abundant ones.[13] For the analysis of co-formulants in vegetable samples at lower limits, an automated headspace solid-phase microextraction (HS-SPME) with gas chromatography coupled to mass spectrometry (GC-MS) could be used since they are normally volatile compounds as naphtha, benzene and toluene compounds. Thus, this technique allows for the preconcentration of the compounds, minimizing sample treatment and reducing experimental errors.[20] On the other hand, liquid chromatography coupled to mass spectrometry (LC-MS) is commonly applied for the determination of myclobutanil and metabolites.[8]

For all of that, the dissipation of myclobutanil and its co-formulants was evaluated in this study under different temperature conditions, room and refrigerated temperatures (22 and 3°C), since it could affect in a different way both myclobutanil dissipation and metabolites' formation, in tomato and grape samples treated with the commercial product Mitrus®. SLE method, employing acetonitrile, was used to extract myclobutanil and metabolites, and ultra-high performance liquid chromatography coupled to high resolution mass spectrometry (UHPLC-Q-Orbitrap-HRMS) was used. For co-formulants, HS-SPME and GC coupled to HRMS (HS-SPME-GC-Q-Orbitrap-HRMS) were employed. Moreover, $^{1}H$ and $^{13}C$ nuclear magnetic resonance (NMR), including 2-D analysis, were used to confirm the structure of a myclobutanil metabolite. Dissipation studies were accomplished during 60 and 80 days for room and refrigerate temperatures respectively. After suspect analysis of parent compound and metabolites, nontargeted analysis was performed to search new metabolites using different software (MassFrontier™ v7.0, Compound Discoverer v3.2 and MassChemSite 3.1.0).

## 2. Materials and methods

136 2.1. Reagents and chemicals

137 Myclobutanil reference standard (purity>99.9%) was obtain from Dr. Ehrenstorfer (Augsburg,
138 Germany). Stock standard solution was prepared at 1000 mg/L in methanol (HPLC grade,
139 Honeywell Riedel-de-Haën (Seelze, Germany)) by weighing 10 mg of solid substance. From this
140 solution, a working standard solution was prepared at 10 mg/L in methanol. Stock and working
141 solutions were stored at -21°C in the dark.

142 Co-formulant analytical standards were: 1,2,4-trimethylbenzene, 1,3,5-trimethylbenzene, 4-
143 isopropyltoluene, ethylbenzene, isopropylbenzene, n-butylbenzene, naphthalene, n-
144 propylbenzene, sec-butylbenzene, styrene, tert-butylbenzene and toluene from Dr.
145 Ehrenstorfer and 2,4-dimethylstyrene, 4-ethyltoluene, 1,3-diisopropylbenzene,
146 pentamethylbenzene, biphenyl, 2-methylbiphenyl, 3-methylbiphenyl, 4-methylbiphenyl and
147 diphenylmethane from Merck (St. Louis, MO, USA).

148 For LC-Q-Orbitrap calibration a mixture of acetic acid, caffeine, Met-Arg-Phe-Ala-acetate salt
149 and Ultramark 1621 (ProteoMass LTQ/FT-hybrid ESI positive) and a mixture of acetic acid,
150 sodium dodecyl sulphate, taurocholic acid sodium salt hydrate and Ultramark 1621 (fluorinated
151 phosphazenes) (ProteoMass LTQ/FT-HybridESI negative), from Thermo-Fisher Scientific, were
152 employed. As exact mass calibrant for GC-Q-Orbitrap analysis, perfluorotributylamine from
153 Thermo Fisher Scientific (Waltham, MD, USA) was used.

154 Acetonitrile was obtained from Honeywell Riedel-de-Haën, water from J.T. Baker (Deventer, The
155 Netherlands), acetic acid from Merck and formic acid (>98% of purity) from Fisher Scientific
156 (Erembodegem, Belgium). Magnesium sulphate was provided by Merck. Deuterated methanol
157 for NMR measurements was obtained from Merck.

158

159 2.2. Instrument and apparatus

160 2.2.1. UHPLC-Q-Orbitrap-HRMS

Thermo Fisher Scientific Vanquish Flex Quaternary LC (Thermo Scientific™, San Jose, CA, USA) was used employing a Hypersil GOLD™ aQ column (100 × 2.1 mm, 1.9 µm particle size) and column temperature was set at 30°C. The chromatographic system was coupled to a hybrid mass spectrometer Q-Exactive Orbitrap (Thermo Scientific Q-Exactive™) working in both positive and negative ionization mode.

Chromatographic and spectrometric parameters are summarized in **Table 1**. To obtain as much information as possible a generic separation method previously optimized was used.[21] Thus, water containing 0.1% formic acid (Eluent A) and methanol (Eluent B) were used as mobile phase, flow rate was set at 0.3 mL/min and the elution gradient was as follow: gradient started with 95% of A and was kept constant for 1 min. Then it decreased to 0% of A in 3 min and kept constant for 6 min. Finally, the percentage of A was increased to 95% in 0.5 min and re-equilibrated during 3.5 min, obtaining a total running time of 14 min. Injection volume was 10 µL. The employed MS parameters were: spray voltage, 4 kV; sheath gas ($N_2$, 95%), 35 (arbitrary units, au); auxiliary gas ($N_2$, 95%), 10 (au); S-lens RF level, 50 (au); heater temperature, 305°C; and capillary temperature, 300°C. The mass spectra were acquired employing: (1) full MS, ESI+ and ESI-, without fragmentation (higher collisional dissociation (HCD) collision cell switched off), mass resolving power = 70,000 Full Width at Half Maximum (FWHM) at *m/z* 200; AGC target = $10^6$; mass range in the full scan experiments was set to *m/z* 60–900; (2) data independent mass spectrometry fragmentation (DIA-MS/MS), ESI+/- (HCD on, collision energy = 30 eV), mass resolving power = 35,000 FWHM at *m/z* 200, AGC target = $2 \cdot 10^5$, isolation window = 50 *m/z*.

The results were acquired using the external calibration mode and they were processed using Xcalibur™ version 4.3.73, with Quan Browser and Qual Browser (Thermo Fisher Scientific, Les Ulis, France) and TraceFinder 5.1 (Thermo Fisher Scientific) for targeted and suspect analysis, whereas MassFrontier™ v7.0, Compound Discoverer v3.2 (Thermo Fisher Scientific) and MassChemSite 3.1.0 (Molecular Discovery Ltd, London, UK) were employed for nontargeted analysis.

187

188 2.2.2. HS-SPME-GC-Q-Orbitrap-HRMS

189 A GC system Thermo Fisher Scientific Trace 1310 with an auto-sampler Triplus RSH (Thermo
190 Scientific™, Thermo Fisher Scientific, San Jose, CA, USA) was used for the analysis of co-
191 formulants. A Varian VF-5ms (30 m x 0.25 mm, 0.25 mm film thickness) supplied by Agilent
192 Technologies (Santa Clara, CA, USA) was employed. Helium (99.9999%) was used as carrier gas
193 at a constant flow rate of 1 mL/min. The GC system operated at an injector temperature of
194 250°C. HS-SPME conditions were: Polydimethylsiloxane (PDMS) SPME fiber, incubation time 1
195 min, extraction time 30 min, incubation temperature 70°C, agitator on 10 s, agitator off 10 s,
196 desorption time 3 min, penetration speed 40 mm/s, needle speed in vial 20 mm/s and flow rate
197 1 mL/min. When the instrument was in standby mode, the injector split ratio was set at 20:1.
198 When the syringe was placed into the injector, splitless mode was switched on for 2 min, and
199 after that, the split valve was open again with a flow rate of 100 mL/min to clean the glass liner
200 and avoid carry-over effects. It was finally reduced to 20 mL/min at 2 min. Septum purge was 5
201 mL/min during the analysis. Column temperature was initially set at 35°C, and it was held for 10
202 min. Then it was increased at 5°C/min to 75°C and at 100°C/min to 300°C, which was held for 10
203 min. The total running time was 30 min. The chromatographic system was coupled to a mass
204 spectrometer Q-Exactive Orbitrap Thermo Fisher Scientific (Q-Exactive™) operating in the
205 electron ionization mode (EI, 70 eV). The Q-Exactive was operated in full scan mode between 50
206 and 500 *m/z*. The temperatures of the transfer line and ionization source were set at 250°C. The
207 analysis was performed with a filament delay of 4 min to prevent instrument damage.
208 The results were acquired using internal calibration mode with the internal standard (IS) styrene-
209 d8 and they were processed using TraceFinder 4.0 (Thermo Fisher Scientific) for suspect analysis
210 of co-formulants. **Table 2** shows the chromatographic and spectrometric parameters employed
211 for co-formulants. Characteristic and fragment ions with their corresponding mass error were
212 obtained from a previous work developed by Maldonado-Reina et al.[12]

213

214 2.2.3. NMR

215 NMR spectra were obtained using a Bruker Avance III HD 600 ($^{1}$H, 600.13 MHz; $^{13}$C, 150.92 MHz)
216 (Bruker Company, Switzerland) with a 5mm QCI quadruple resonance pulse field gradient
217 cryoprobe, giving the chemical shifts in ppm, relative to the residual solvent signal. Standard
218 Bruker pulse programs were used for the acquisition of the NMR spectra. $^{1}$H acquisition
219 parameters were: NS = 4 scans, DS = 2 scans, size of FID = 65536, FID resolution = 0.22 Hz,
220 spectral width = 12.02 ppm, acquisition time = 4.54 s, relaxation delay = 5 s, receiver gain = 18.
221 $^{13}$C acquisition parameters were: NS =6144 scans, DS = 0 scans, size of FID = 65536, FID resolution
222 = 1.16 Hz, spectral width = 250.9 ppm, acquisition time =0.87 s, relaxation delay = 5 s, receiver
223 gain = 203. q, quintuplet and m, multiplet were the abbreviations used to indicate the
224 multiplicity of signals. The following experiments were conducted: $^{1}$H-NMR, $^{13}$C-NMR, ($^{1}$H-$^{1}$H)-
225 COSY, ($^{1}$H-$^{13}$C)-HMQC and ($^{1}$H-$^{13}$C)-HMBC.
226 The results were acquired using an internal calibration with trimethylsilyl propionic acid (TMSP)
227 (Eurisotop, Saarbrücken, Germany) and they were processed using TopSpin 4.0.7 (Bruker).
228

229 2.3. Dissipation assays

230 Tomato and grape blank samples were obtained from an organic local store in Almería, Spain.
231 Ten kg of each sample was sprayed with Mitrus® (myclobutanil 12.5%, EC) at the manufacturer
232 recommended dose (0.06% for tomato and 0.08% for grape). After that they were divided in two
233 groups and stored at room (22°C) and refrigerator temperature (3°C) to simulate how pesticides
234 are degraded after harvest. Samples were analysed at different periods of time after application:
235 2 h, 6 h, 1 day, 2 days, 5 days, 12 days, 20 days, 30 days, 40 days, 50 days and 60 days for room
236 and refrigerated temperature, and 70 days and 80 days for refrigerated temperature as well.
237 Two samples of each matrix and for each temperature were used as a control of water weight

loss and the concentrations of dissipation assay were calculated taking into account this loss of mass.

### 2.4. Sample treatment

In the case of the analysis of active substance and metabolites, a generic SLE method employing acetonitrile was used, since it allows the extraction of both polar and medium polarity compounds. Briefly, 5 g of sample was weighed in a 50 mL polypropylene tube and agitated with 5 mL of acetonitrile during 1 min. The tubes were centrifuged at 7500 rpm (8170 rcf) and the extract was transferred to a vial prior the UHPLC-Q-Orbitrap-HRMS analysis. In the case of grape samples, the layer of water and acetonitrile was separated after centrifugation, as it can be observed in **Figure S1**.

For the analysis of co-formulants, HS-SPME-GC-Q-Orbitrap-HRMS was employed. The HS-SPME method was as follow: 5 g of sample was weighed in a SPME vial, and the IS (styrene-D8) was added at 50 µg/kg to all samples, to normalize the signals. The samples were agitated for 1 min in vortex to homogenised them and submitted to the analysis, according to the conditions described in *Section 2.2.2*.

## 3. Results and discussion

### 3.1. Method optimization

#### 3.1.1. UHPLC-Q-Orbitrap-HRMS optimization

MS characterization was only performed for myclobutanil. In the case of known metabolites, exact masses were calculated according to their molecular formula, and it was employed during the tentative identification stage. All compounds were identified using a mass error lower than 5 ppm for the characteristic and fragment ions, and at least one fragment ion should be detected with a variability in isotopic pattern recognition of the characteristic ion less than 30%.[22]

A generic gradient previously developed was employed to separate the maximum number of compounds as possible.[21] Mobile phases were slightly different, being methanol and water containing 0.1% formic acid. Myclobutanil eluted at 7.95 min (**Figure S2**). Fragments were proposed using MassFrontier™ v7.0 software and the fragmentation occurs more easily in the α or β-carbon near to the chlorobenzene. For the optimization of the extraction method, grape and tomato were evaluated. QuEChERS extraction was not tested since polar compounds as polar metabolites of triazole compounds were not extracted.[8] Thus, two SLE methods were checked. For the first one, acetonitrile was selected as extractant solvent, whereas for the second one, methanol acidified with acetic acid (0.5% *v/v*) was tested, which allows the extraction of the most polar compounds.[23] Recoveries at 5 (for grape) or 10 µg/kg (for tomato), using methanol as extraction solvent, were between 113-126% (RSD=2.9-3.5%), while when acetonitrile was used, recoveries ranged from 99 to 110% with RSD between 1 and 12% (**Table S1**). Performance was slightly better when acetonitrile was used, and lower matrix effect was achieved (matrix effect has been calculated using the formula of the Lopez-Ruiz et al. study),[24] ranging from -17 to -31%, whereas when methanol was used, it ranged from -32 to -67%. Therefore, SLE with acetonitrile was chosen as the final extraction method.

3.1.2. HS-SPME-GC-Q-Orbitrap-HRMS

For the analysis of co-formulants, first a liquid injection was tested for the compounds included in **Table S2**. To do that, two SLE methods were employed, using 10 g of tomato and 10 mL of the extraction solvent. The extraction solvents tested were ethyl acetate and *n*-hexane. After 1 min of agitation in vortex and centrifugation, 0.15 g of magnesium sulfate was added to 1.5 mL of supernatant for water removal. Subsequently, 1 min of vortex agitation and centrifugation were performed and the final extract was injected in the GC-Q-Orbitrap-HRMS system, using an injection volume of 2 µL. For ethyl acetate, recoveries ranged from 62 to 85% with RSDs lower

than 10% and matrix effect between -16-27%, while for *n*-hexane, recoveries were from 82-109% with RSD values lower than 6%, and matrix effect ranged from 6-30%.

Although validation parameters were optimal for both methods, limits of quantification were generally too high (5-25 µg/kg) for the expected concentrations of co-formulants in samples (**Table S2**). For that, a HS-SPME extraction previously developed and validated (recoveries ranged 70-120%) in the researcher group was applied. Conditions are described in *Section 2.2.2.*

3.2. Method validation

The method was validated for myclobutanil analysis (SLE and UHPLC-HRMS methodology) following the parameters proposed by SANTE guideline.[22] The parameters evaluated were linearity, matrix effect, limit of quantification (LOQ), trueness in term of recoveries and precision (**Table S1**).

Linearity was evaluated injecting a matrix-matched calibration, spiking blank extracted samples at the concentration of 2.5, 5, 10, 25, 50, 100, 250 and 500 µg/kg. Regression coefficients were higher than 0.9956 in a linear range between 2.5 and 250 µg/kg. Working range was set between 5 and 100 µg/kg.

Matrix effect was determined by comparison between the matrix-matched calibration used for linearity with a solvent calibration at the same concentrations. It ranged from -17 for tomato to -31% for grape, so matrix match calibrations were prepared in both matrices for quantification purposes.

LOQs were stablished as the minimum concentrations at which both precursor and product ions were observed with a signal to noise ratio higher than 10 and with trueness and precision values between 70-120% and lower than 20% respectively. LOQs ranged from 5 to 10 µg/kg, for grape and tomato respectively.

312 Recoveries were calculated spiking blank samples at concentrations of 5 µg/kg for grape or 10
313 µg/kg for tomato and 100 µg/kg, and it ranged from 99 to 110% with intra and interday precision,
314 in term of RSDs, of 1-9% and 4-12% respectively.
315
316 3.3 Myclobutanil dissipation
317 Approximately 0.3 kg of tomato and 0.1 kg of grape were collected and crushed at the
318 mentioned time intervals after Mitrus® application, as described in *Section 2.3*. Myclobutanil
319 dissipation in tomato and grape at 22°C and 3°C was fitted to a biphasic kinetic model (Equation
320 1),[25]
321 $C(t) = C_0\,(a\,e^{-k_1 t_1} + (1-a)e^{-k_2 t_2})$ (1)
322 where $k_1$ and $k_2$ are the constant rates, $a$ is the fraction of the initial chemical that degrades at
323 the fast rate, $C_0$ is the initial concentration and $C(t)$ is the concentration at time $t$. Residual level
324 ($RL_{50}$) was also estimated using Equation 2.
325 $RL_{50} = \frac{\ln 2}{k}$, where $k$ could be $k_1$ or $k_2$ (2)
326 Parameters are indicted in **Table 3** and the dissipation graphs of myclobutanil are shown in
327 **Figure 1** for tomato and **Figure S3** for grape. Similar adjustments were obtained in other studies
328 although for different compounds.[26] It is important to mention that other kinetic models as zero
329 order, half order, first order or second order [25,27] were tested, and the best fit was achieved with
330 a biphasic model ($R^2$>0.95 in all cases).
331 It can be seen that in **Figure 1** and **Figure S3** the concentration of myclobutanil in the first hours
332 after application increased for both, grape and tomato samples. Then the concentration
333 achieved a maximum and later decreased slowly. This maximum concentration was reached
334 after 5 (tomato at 22°C), 12 (grape at 22 and 3°C) and 20 days (tomato at 3°C). The obtained
335 concentrations in grape were higher than in tomato, probably due to the morphology of grape
336 that kept a higher volume of PPP solution than tomato. In both samples, dissipation was lower
337 at 3°C, being the difference much bigger in tomato samples. Besides, after 60 days, at 22°C

myclobutanil had almost disappeared (9% for tomato and grape), while at 3°C, even after 80 days myclobutanil remained at the 20% of the highest concentration for tomato and 18% for grape. Nevertheless, the samples were not in the optimal conditions to be consumed so continuing their analysis was meaningless. Biphasic kinetic model revealed that in the case of tomato at both temperatures and in grape at 22°C, $k_1$ and $k_2$ were similar, indicating that the dissipation rate was similar in both phases. However, in grape stored at 3°C, $k_1$ was lower at the first phase (0.0012 $hours^{-1}$) and higher at the second phase (0.0053 $hours^{-1}$). These results were reflected in the $RL_{50}$, that was 24 days at the first phase and 5.5 days at the second phase. $RL_{50}$ values for the other conditions and matrices are shown in **Table 3**, and they ranged from 10 to 15 days in all cases.

Comparing these results with Pesticide Properties DataBase (PPDB) web,[6] myclobutanil has a dissipation rate $RL_{50}$ on and in plant matrix from 2.3 to 10.5 days, which are slightly lower than those obtained in this study, but this can be attributed to the type of matrix which is not indicated in PPDB web. $RL_{50}$ at refrigerate temperature in grape is lower than the indicated in PPDB (92 days). In relation to other previous published studies, Sun et al.[28] evaluated the kinetic dissipation of myclobutanil in strawberry, obtaining a $RL_{50}$ of 5.78 days, whereas in this study myclobutanil dissipated more slowly in tomato and grapes. Salunke et al.[29] obtained $RL_{50}$ values in accordance with those obtained in this work (9.93-10.59), ranging from 12.4-12.6 days in the case of grapes. Finally, Hlihor et al.[30] determined the dissipation of myclobutanil in tomatoes with $RL_{50}$ values of 48.59 days when commercial product was applied at recommended dose, and when the commercial product was applied at double douse, $RL_{50}$ was 1.28 days. This value is different to those obtained in other matrices and studies, so it cannot be comparable with our study in tomato.

### 3.4. Myclobutanil metabolites

Metabolites may be as toxic as parent compounds (or even more toxic). For that, in addition to myclobutanil, its metabolites were searched through a suspect screening.

Apart from the metabolites described in bibliography, nontargeted analysis was done to search unknown myclobutanil's metabolites. The degraded samples were processed using the software MassChemSite 3.1.0, which exposed possible metabolites in the samples based on different organic and inorganic reactions, providing the exact mass of these possible metabolites. Thus, 11 metabolites were putatively identified for myclobutanil and included in the in-house database to search them in all the samples (**Table 1**). Then, in order to achieve a correct identification, different factors were taken into consideration: expected retention times, as for example, common triazole metabolites will have lower retention times in reverse phase columns; isotopic pattern, concretely for those myclobutanil metabolites which keep the chlorine atom, and fragmentation pattern similar to parent compounds. That last point was performed using MassFrontier™v7.0 software. **Figure 2** and **Figures S4.1**, **S4.2**, **S4.3**, **S4.4** and **S4.5** show the identified compounds in the samples following the methodology previously mentioned, including the extracted ion and fragment ion chromatograms for each of them. The compounds RH-9089 and RH-9090 have in common the fragment 125.0154 *m/z,* but as they have other fragment ions to confirm them, both compounds could be clearly identified. Moreover, 7, 9, 10 and 11-myclobutanil metabolites (**Figure 3**) were described and detected in samples for the first time. As they are not described in bibliography, their structures were putatively assigned, using the program MassChemSite 3.1.0. Thus, 7-myclobutanil can be formed by oxidation of nitrile and chlorine group to a carbonyl and hydroxy group, 9-myclobutanil by glycosylation of the benzene ring, 10-myclobutanil by oxidation of nitrile to a carbonyl group and 11-myclobutanil by reduction and formation of a double bond in the alkyl chain. The metabolite TA was detected only at 2h in grape at 22°C and at very low concentration, so no fragments could be extracted in the sample.

388 It is important to mention that although there was no data about metabolite toxicity, using the
389 tool T.E.S.T. Version 5.1.1 of the Environmental Protection Agency (EPA), estimated toxicity for
390 both known and unknown metabolites could be theoretically calculated. As it can be seen in
391 **Table 1**, some lethal doses in rats are shown, although unknown metabolites structures could
392 differ from their actual structures. In some cases, as for RH-9089 (730.81 mg/kg), 9-myclobutanil
393 (242.55 mg/kg) and 10-myclobutanil (899.82 mg/kg) lower amounts were obtained compared
394 to parent compound (1601.81 mg/kg), indicating that these compounds could be more toxic
395 than myclobutanil.
396 Once the compounds in the database were confirmed or discarded according to the factors
397 explained above, their evolutions along the degradation study were evaluated, using the signal
398 of myclobutanil for quantification purposes (**Figure 1** and **Figure S3** as well as in **Table S3.1** and
399 **S3.2**). While RH-9090, 9-myclobutanil and 10-myclobutanil were the main metabolites, RH-9089,
400 7-myclobutanil and 11-myclobutanil were detected at lower concentrations. Generally, all the
401 metabolites followed the same trend, and after 30 days, the maximum concentration was reach,
402 corresponding with the decreasing of myclobutanil concentration (after 20 days). Besides, after
403 70-80 days their concentration increased, corresponding to the lowest myclobutanil
404 concentration. Particularly, RH-9089 appeared after 20 days since it was formed from RH-9090
405 (which begins to appear at 2 hours).[7] Whereas 7-myclobutanil was only detected in tomato at 5
406 days, 1-myclobutanil was only identified in grape from 1 day to 40 days after application. Finally,
407 10-myclobutanil was found in all the treated samples and it can be detected even in the standard
408 solution.
409
410 3.5. NMR “10-myclobutanil” metabolite confirmation
411 The case of 10-myclobutanil metabolite is a special issue. It was detected even in the calibration
412 curve and in a solvent standard-point only containing myclobutanil, with an area 30 times lower
413 than myclobutanil. Using the software MassChemSite 3.1.0 a structure where the nitrile group

414 was substituted for an aldehyde group was proposed. In order to confirm the structure of the
415 10-myclobutanil metabolite in the standard solution, this was analysed by $^{1}H$ and $^{13}C$ NMR.
416 Samples were prepared dissolving 5 mg of myclobutanil standard in 5 mL of deuterated
417 chloroform ($CDCl_3$). The sample was measured immediately after preparation and after 14 days
418 at room temperature to accelerate the possible degradation into 10-myclobutanil. $^{1}H$ NMR
419 measure revealed that the aldehyde signal did not appear in the measurement. Considering the
420 number of unsaturations provided by Xcalibur software (RBD), 7.5, another structure was
421 proposed. In this structure (**Figures 4** and **S4.5**) the nitrile was substituted by a carbonyl group
422 and the alkyl chain forms a cycle, not existing the aldehyde hydrogen.
423 As it can be observed in **Figure 4**, although the signal did not match perfectly with the estimated
424 chemical shift of ChemDraw Professional 16.0, there was a good correlation between them.
425 Besides, it can clearly be seen that some signals appear after 14 days of standard preparation.
426 The main signals were assigned as: $^{1}H$ NMR (600.13 MHz, $CDCl_3$, δ, ppm) 3.22-3.24 (2H, m, C3,
427 $CH_2$), 2.46-2.48 (2H, m, C8, $CH_2$), 1.70-1.82 (2H, q, C6, $CH_2$), 1.62-1.68 (4H, m, C5 y C8, 2x$CH_2$) and
428 $^{13}C$ NMR (150.92 MHz, $CDCl_3$, δ, ppm) 175.20 (C9) , 42.12 (C3), 42.06 (C4), 35.73 (C8), 30.06 (C6),
429 29.10 (C7), 22.93 (C5). The ketone carbon (C9) only appeared as a small signal because the
430 carbon is only linked to an oxygen and the estimated concentration is too low to see it clearly
431 (≈30 mg/L).
432 To confirm the proposed structure, 2D-NMR experiments were performed: ($^{1}H$-$^{1}H$)-COSY, ($^{1}H$-
433 $^{13}C$)-HMQC and ($^{1}H$-$^{13}C$)-HMBC. It has to be mentioned that metabolites concentration was very
434 low in comparison with parent compound, making the assignation more difficult, and therefore
435 not all the correlations could be assigned, showing the results in **Figures S5**, **S6** and **S7**. In ($^{1}H$-
436 $^{1}H$)-COSY experiment (**Figure S5**), correlation between protons H8-H7 and H7/H5-H6 can be
437 seen. ($^{1}H$-$^{13}C$)-HMQC experiment was performed to see close correlation between $^{1}H$ and $^{13}C$
438 signals. Correlation between C5-H5, C7-H7, C8-H8 and C3-H3 are assigned in **Figure S6**. Finally,
439 through ($^{1}H$-$^{13}C$)-HMBC distant correlation between $^{1}H$ and $^{13}C$ signals can be seen. In **Figure**

**S7.1**, correlations between C5-H7 and C7-H5 (2 carbons away), C8-H6 and C6-H8 (2 carbons away), C8-H5 and C5-H8 (3 carbons away) and C6-H3 (3 carbons away) can be assigned. In **Figure 7.2**, the correlation between C9-H3 and C9-H7 can be observed, as a small signal, which confirms the presence of a ketone group, which appeared as a small signal in the $^{13}C$ NMR experiment.

### 3.6. Co-formulants

To search co-formulants in the tomato samples applied with the PPP Mitrus®, an in-house database previously developed was used (**Table 2**).[12] As both myclobutanil and metabolites have a similar behaviour in tomato and grape, co-formulants were only determined in incurred tomato samples. Using the HS-SPME-GC-HRMS method, seven compounds were confirmed directly in tomato samples: 1,2,4-trimethylbenzene, mesitylene, 2-methyl-biphenyl, biphenyl, naphthalene, pentamethylbenzene, tert-butylbenzene. Benzene derivative detected compounds can cause different health problems as skin, eyes and respiratory irritation and they could have narcotic and toxic effects as naphthalene or pentamethylbenzene compounds.[12] They can also be toxic to aquatic life. Although detected compounds are normally introduced in the body through inhalation, some of them as 1,2,4-trimethylbenzene or mesitylene are readily absorbed by oral exposure.[31] This highlights the importance of having analytical methods to determine both active substances from PPPs and other constituents, as well as to monitor them in real samples.

The compounds were quantified, and dissipation curves were calculated along 2 h, 6 h, 1 day, 2 days, 5 days and 12 days at 3 and 22°C in tomato (**Figure 5**). The detected compounds were found at lower concentrations than myclobutanil, being the highest concentration of 71 µg/kg for the sum of 2-methyl-biphenyl and 3-methyl-biphenyl (which were not separated using the GC conditions applied). Besides, all the compounds rapidly decreased until 12 days after application being the dissipation slower at 3°C. The highest concentrations after 12 days were at 2.6 and 2.1 µg/kg for tert-butylbenzene and naphthalene respectively at 3°C.

To conclude, this study evaluates the dissipation of myclobutanil in in-lab treated tomato and grape samples under different temperatures, ambient (22°C) and refrigerated (3°C), being dissipation slower for refrigerated conditions. A wide variety of analytical tools were employed to monitor myclobutanil and dissipation of co-formulants, including SLE and HS-SPME as extraction methods and UHPLC-Q-Orbitrap-HRMS and GC-Q-Orbitrap-HRMS as analytical techniques. The results shown that, after a first increasing, myclobutanil dissipation was similar at 22°C for both tomato and grape samples following a biphasic kinetic model, with $RL_{50}$ (both $RL_{50\ K1}$ and $RL_{50\ K2}$) from 10 to 12 days respectively. At 3°C degradation it was lower, being $RL_{50}$ around 15 days for tomato (for both $RL_{50\ K1}$ and $RL_{50\ K2}$) whereas in grape, $RL_{50\ K1}$ was 24 days while $RL_{50\ K2}$ was 5 days, so although $RL_{50\ K2}$ was lower at 22°C, the overall dissipation is higher at 22 ºC.

Myclobutanil metabolites were searched in the incurred samples. In addition to known metabolites, unknown metabolites obtained from in-silico software as MassChemSite 3.1.0 were found. Four myclobutanil metabolites, not described previously in bibliography, were putatively identified and one of them was also analysed by $^{1}H$ and $^{13}C$ NMR as confirmation tool, indicating the need of applying several tools to perform a comprehensive characterization of dissipation processes. In addition, co-formulants of Mitrus® were also identified and quantified in tomato samples. Seven compounds were identified directly in tomato samples, being the first time they are found in samples after application at such low concentrations. After identification, dissipation curves of myclobutanil metabolites and co-formulants were estimated. Myclobutanil metabolites were formed during myclobutanil dissipation, observing a clear increasing for all of them at 80 days after plant protection product application and in the case of co-formulants, they degraded almost completely 12 days after application.

**Supporting Information description**

Supporting information associated with this article can be found in the online version.

**Acknowledgements**

Authors gratefully acknowledge to the Regional Government of Andalusia, Spain for financial support (project reference: P18-RT-2329). RLR acknowledges to the Andalusian Ministry of Economic Transformation, Industry, Knowledge and Universities for financial support from "Ayudas para Captación, Incorporación y Movilidad de Capital Humano de I+D+i (PAIDI 2020)".

**Figure caption**

**Figure 1.** Concentration of the parent compound (adjusting to kinetic model "biphasic kinetic'') and degradation curves for myclobutanil metabolites in tomato

**Figure 2.** Extracted ion and fragment ion chromatograms of 11-myclobutanil metabolite after 30 days of Mitrus® application at 3°C

**Figure 3.** Myclobutanil metabolites detected in real samples

**Figure 4**. $^{1}H$ NMR for a 1000 mg/L myclobutanil standard solution after 0 days (A) and 14 days (B) and $^{13}C$ NMR for a 1000 mg/L myclobutanil standard solution after 0 days (C) and after 14 days (D). Shifts in green are estimated by ChemDraw Professional 16.0, while in purple are experimental values.

**Figure 5.** Dissipation curve for co-formulants in tomato

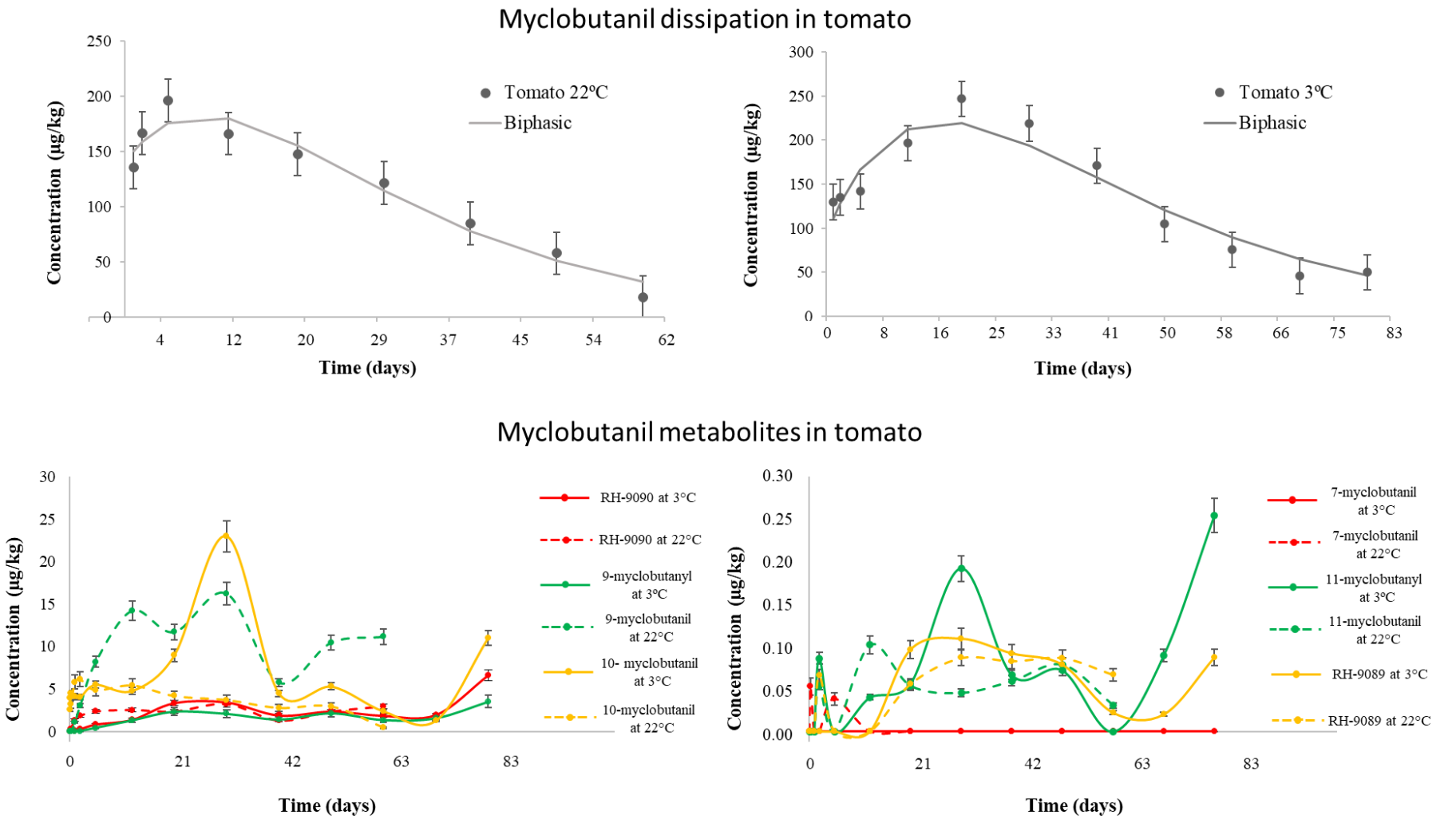


**Figure 1.** Concentration of the parent compound (adjusting to kinetic model "biphasic kinetic'') and degradation curves for myclobutanil metabolites in tomato

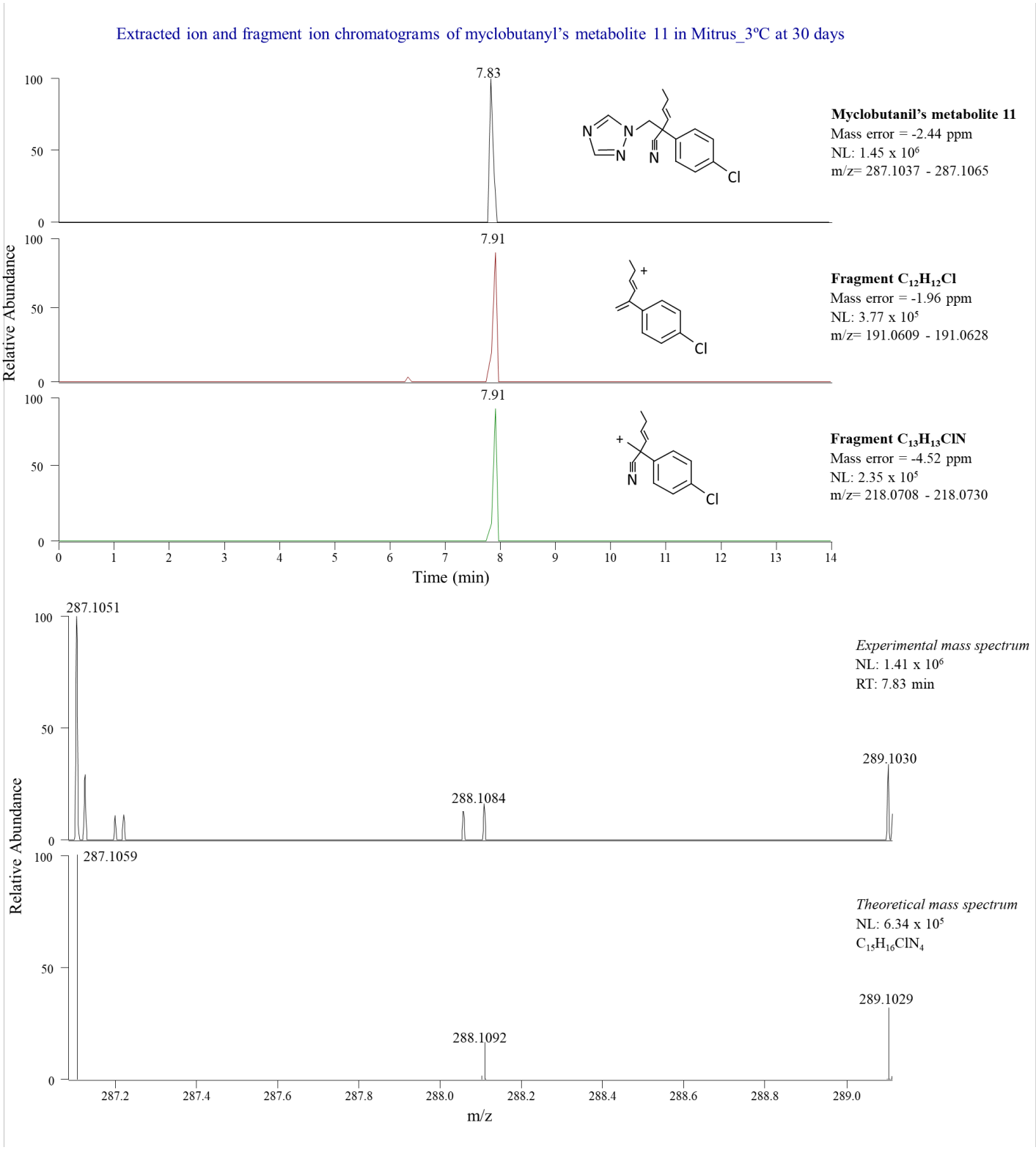


**Figure 2.** Extracted ion and fragment ion chromatograms of 11-myclobutanil metabolite after 30 days of Mitrus® application at 3°C

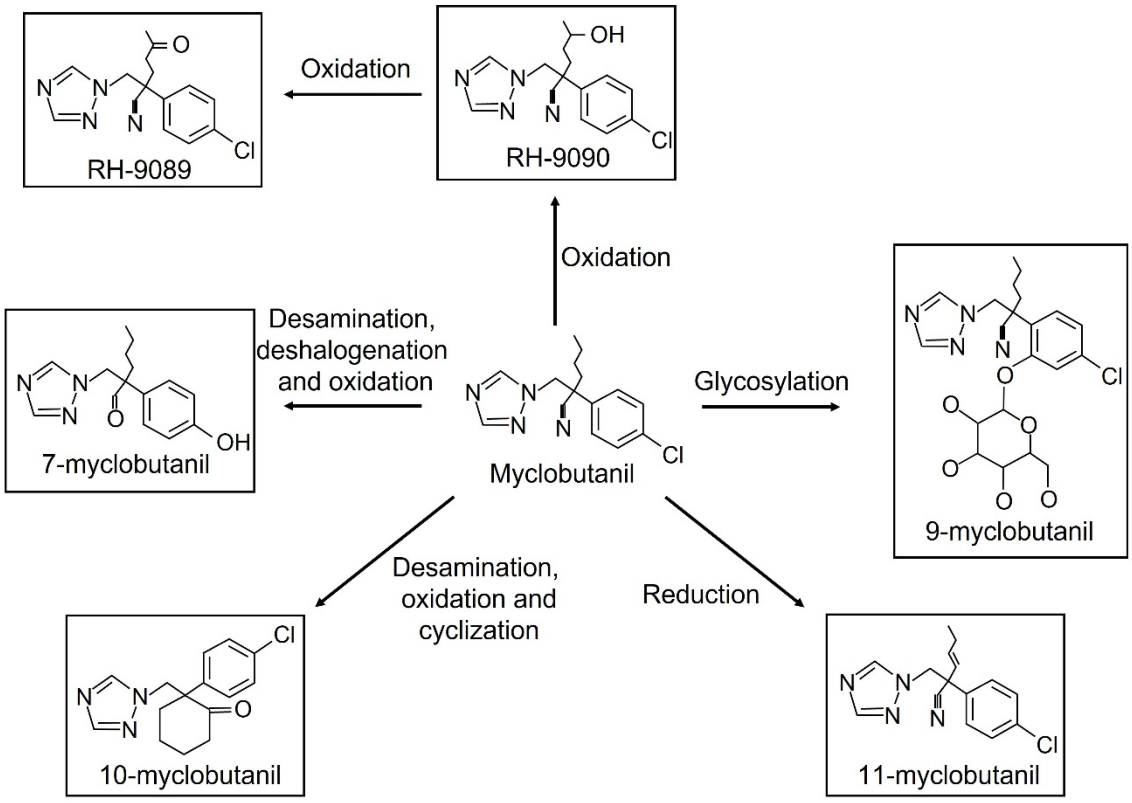


**Figure 3.** Myclobutanil metabolites detected in real samples

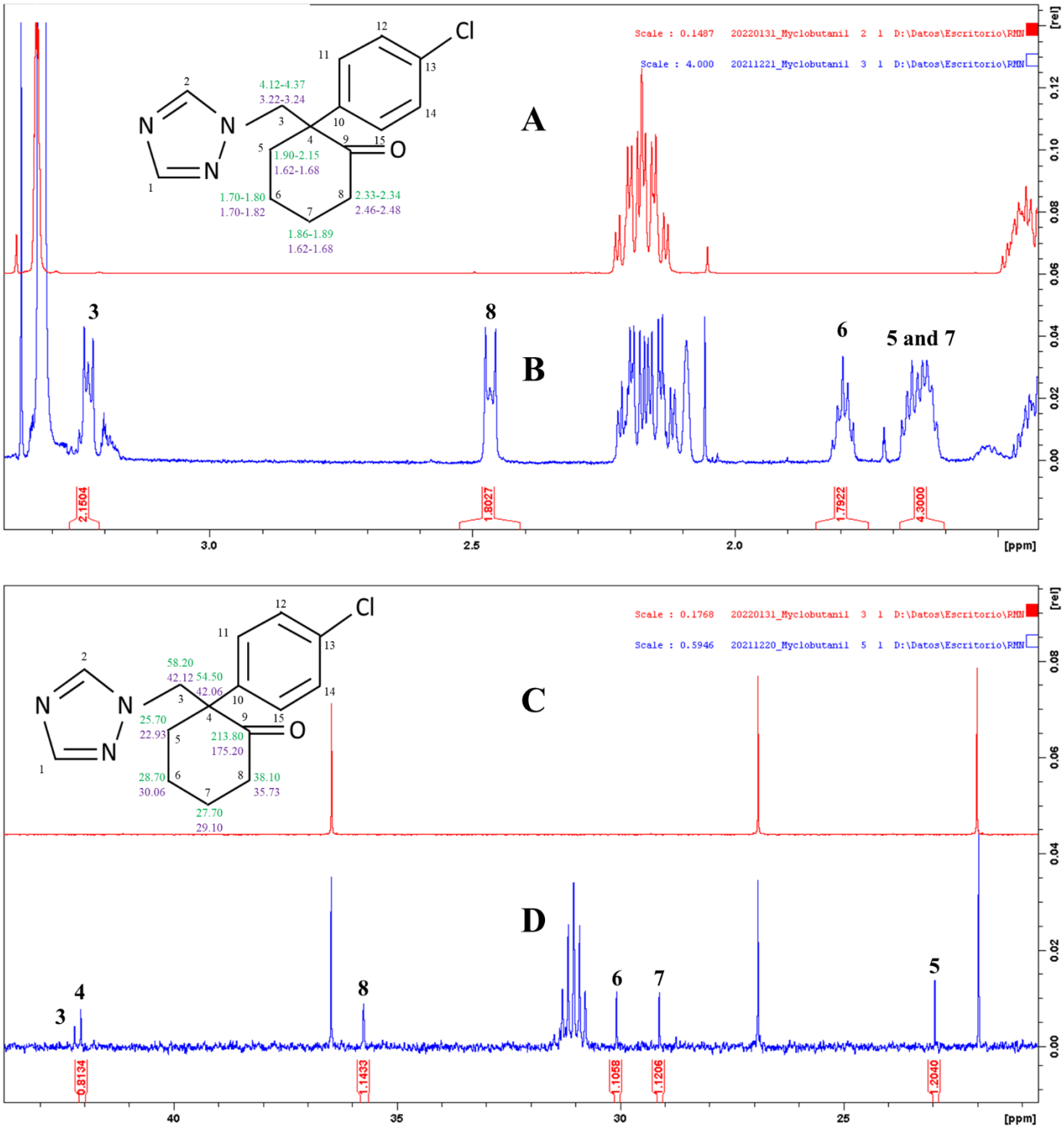


**Figure 4**. $^{1}$H NMR for a 1000 mg/L myclobutanil standard solution after 0 days (A) and 14 days (B) and $^{13}$C NMR for a 1000 mg/L myclobutanil standard solution after 0 days (C) and after 14 days (D). Shift in green are estimated by ChemDraw Professional 16.0, while in purple are experimental values.

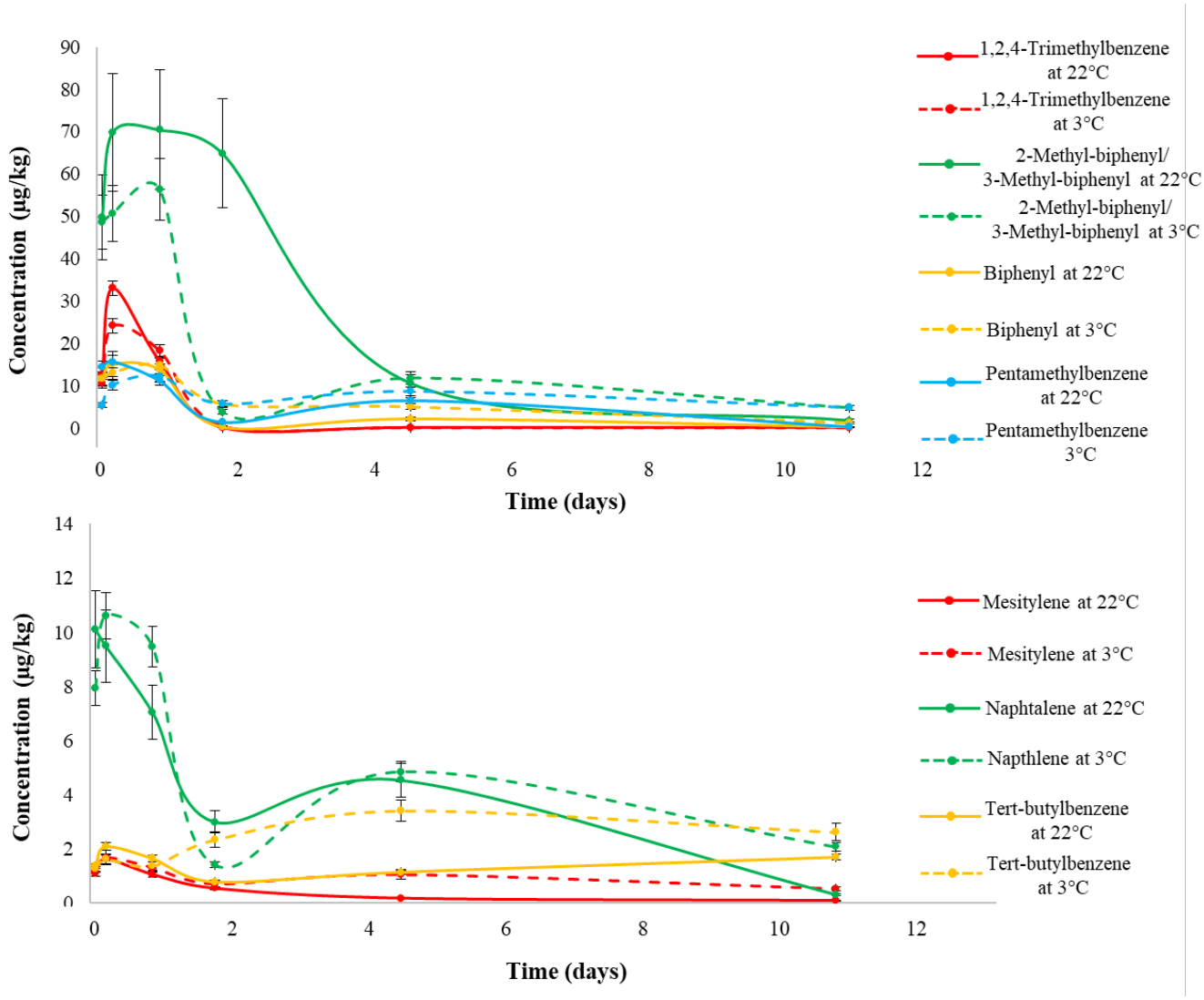


**Figure 5.** Dissipation curve for co-formulants in tomato

**Table 1:** UHPLC-Q-Orbitrap-HRMS parameters for targeted and suspect compounds

| Compound | | RTW (min)* | Predicted oral rat LD50 (mg/kg) | Neutral exact mass | Neutral formula | Precursor ion | | | Fragment ions | | | Ref. |
|---|---|---|---|---|---|---|---|---|---|---|---|---|
| | | | | | | $[M+H]^+$ Theoretical exact mass (*m/z*) | $[M+H]^+$ molecular formula | Mass error (ppm) | Theoretical exact mass (*m/z*) | $[M+H]^+$ molecular formula | Mass error (ppm) | |
| **Target compounds** | | | | | | | | | | | | |
| Myclobutanil | | 7.90-7.98 | 1601.81[#] | 288.1136 | $C_{15}H_{17}ClN_4$ | 289.1215 | $C_{15}H_{18}ClN_4$ | -1.14 | 125.0153 | $C_7H_6Cl$ | -1.64 | - |
| | | | | | | | | | 193.0773 | $C_{12}H_{14}Cl$ | -3.08 | |
| | | | | | | | | | 220.0880 | $C_{13}H_{15}ClN$ | -1.08 | |
| **Suspect compounds** | | | | | | | | | | | | |
| Myclobutanil metabolites described in bibliography | Triazol | - | - | 69.0322 | $C_2H_3N_3$ | 70.0400 | $C_2H_4N_3$ | - | - | - | - | [8] |
| | TAA | - | - | 127.0376 | $C_4H_5N_3O_2$ | 128.0455 | $C_4H_6N_3O_2$ | - | - | - | - | |
| | TA | 1.52 | - | 156.0642 | $C_5H_8N_4O_2$ | 157.0720 | $C_5H_9N_4O_2$ | - | - | - | - | |
| | TLA | - | - | 157.0482 | $C_5H_7N_3O_3$ | 158.0560 | $C_5H_8N_3O_3$ | - | - | - | - | |
| | RH-9090 | 7.08-7.11 | 1603.90 | 304.1085 | $C_{15}H_{17}ClN_4O$ | 305.1164 | $C_{15}H_{18}ClN_4O$ | -0.61 | 125.0154 | $C_7H_6Cl$ | 0.92 | [7,9] |
| | | | | | | | | | 209.0728 | $C_{12}H_{14}ClO$ | -1.34 | |
| | | | | | | | | | 236.0837 | $C_{13}H_{15}ClNO$ | -4.75 | |
| | RH-9089 | 7.04-7.11 | 730.81 | 302.0929 | $C_{15}H_{15}ClN_4O$ | 303.1007 | $C_{15}H_{16}ClN_4O$ | -1.04 | 125.0154 | $C_7H_6Cl$ | 1.01 | |
| | | | | | | | | | 207.0571 | $C_{12}H_{12}ClO$ | -4.78 | |
| | RH-0294 | - | - | 320.1040 | $C_{15}H_{17}ClN_4O_2$ | 321.1118 | $C_{15}H_{18}ClN_4O_2$ | - | - | - | - | |
| | M1 | - | - | 318.0878 | $C_{15}H_{15}ClN_4O_2$ | 319.0956 | $C_{15}H_{16}ClN_4O_2$ | - | - | - | - | |

| | | | | | | | | | | | | |
|---|---|---|---|---|---|---|---|---|---|---|---|---|
| | M2 | - | - | 321.0875 | $C_{15}H_{16}ClN_3O_3$ | 322.0953 | $C_{15}H_{17}ClN_3O_3$ | - | - | - | - | |
| In-silico myclobutanil metabolites | 1-Myclobutanil | - | - | 364.1297 | $C_{17}H_{21}ClN_4O_3$ | 365.1353 | $C_{17}H_{22}ClN_4O_3$ | - | - | - | - | MassChemSite |
| | 2-Myclobutanil | - | - | 254.1526 | $C_{15}H_{18}N_4$ | 255.1586 | $C_{15}H_{19}N_4$ | - | - | - | - | |
| | 3-Myclobutanil | - | - | 432.2003 | $C_{21}H_{28}N_4O_6$ | 433.2076 | $C_{21}H_{29}N_4O_6$ | - | - | - | - | |
| | 4-Myclobutanil | - | - | 252.1370 | $C_{15}H_{16}N_4$ | 253.1428 | $C_{15}H_{17}N_4$ | - | - | - | - | |
| | 5-Myclobutanil | - | - | 346.1191 | $C_{17}H_{19}ClN_4O_2$ | 347.1303 | $C_{17}H_{20}ClN_4O_2$ | - | - | - | - | |
| | 6-Myclobutanil | - | - | 348.1348 | $C_{17}H_{21}ClN_4O_2$ | 349.1426 | $C_{17}H_{22}ClN_4O_2$ | - | - | - | - | |
| | 7-Myclobutanil | 7.24-7.30 | - | 273.1472 | $C_{15}H_{19}N_3O_2$ | 274.1527 | $C_{15}H_{20}N_3O_2$ | -3.49 | 107.0491 | $C_7H_7O$ | 0.45 | |
| | | | | | | | | | 205.1216 | $C_{13}H_{17}O_2$ | -3.30 | |
| | 8-Myclobutanil | - | - | 270.1475 | $C_{15}H_{18}N_4O$ | 271.1532 | $C_{15}H_{19}N_4O$ | - | - | - | - | |
| | 9-Myclobutanil | 6.83-6.89 | 242.55 | 466.1614 | $C_{21}H_{27}ClN_4O_6$ | 467.1680 | $C_{21}H_{28}ClN_4O_6$ | -2.55 | 287.1061 | $C_{15}H_{16}N_4Cl$ | 0.87 | |
| | | | | | | | | | 329.0754 | $C_{15}H_{18}ClO_6$ | -5.76 | |
| | 10-Myclobutanil | 7.90-7.95 | 899.82 | 291.1133 | $C_{15}H_{18}ClN_3O$ | 292.1200 | $C_{15}H_{19}ClN_3O$ | -0.09 | 141.0113 | $C_7H_6ClO$ | 5.88 | |
| | | | | | | | | | 223.0886 | $C_{13}H_{16}ClO$ | 0.59 | |
| | 11-Myclobutanil | 7.78-7.83 | 1597.37 | 286.0980 | $C_{15}H_{15}ClN_4$ | 287.1051 | $C_{15}H_{16}ClN_4$ | -2.44 | 191.0622 | $C_{12}H_{12}Cl$ | -1.96 | |
| | | | | | | | | | 218.0719 | $C_{13}H_{13}ClN$ | -4.52 | |

Abbreviations: RTW=Retention time window; TAA=Triazolylacetic acid; TA=Triazolylalanine; TLA=Triazole lactic acid

*Compounds with – were not detected

[#]Experimental oral rat LD50 (mg/kg) [9]

**Table 2:** GC-Q-Orbitrap-HRMS parameters for the suspect co-formulants. Data obtained from Maldonado-Reina et al [12].

| Compound | RTW (min)* | Molecular formula | Characteristic ion | | Fragment ions | |
|---|---|---|---|---|---|---|
| | | | Theoretical exact mass (*m/z*) | Mass error (ppm) | Theoretical exact mass (*m/z*) | Mass error (ppm) |
| 1,2,4-Trimethylbenzene | 18.52-18.63 | $C_9H_{12}$ | 120.0939 | -4.90 | 105.0704 | -5.80 |
| | | | | | 119.0861 | -4.53 |
| Mesitylene | 18.42-18.46 | $C_9H_{12}$ | 120.0939 | -2.83 | 105.0704 | -3.62 |
| | | | | | 119.0861 | -1.09 |
| 2-Methyl-biphenyl/ 3-Methyl-biphenyl | 20.60-20.95 | $C_{13}H_{12}$ | 168.0939 | -4.82 | 167.0861 | -4.13 |
| | | | | | 165.0704 | -3.76 |
| Biphenyl | 20.31-20.53 | $C_{12}H_{10}$ | 154.0783 | -4.80 | 153.0704 | -4.25 |
| | | | | | 152.0626 | -3.81 |
| Naphthalene | 19.85-19.96 | $C_{10}H_8$ | 128.0626 | -4.69 | 126.0470 | -3.94 |
| | | | | | 102.0464 | -3.89 |
| Pentamethylbenzene | 20.11-20.36 | $C_{11}H_{16}$ | 148.1252 | -4.32 | 147.1174 | -3.87 |
| | | | | | 133.1017 | -4.51 |
| Tert-butylbenzene | 18.33-18.55 | $C_{10}H_{14}$ | 134.1096 | -3.80 | 119.0861 | -4.79 |
| | | | | | 91.0548 | -6.48 |
| p-Cymene | - | $C_9H_{12}$ | 120.0939 | - | - | - |
| Ethylbenzene | - | $C_8H_{10}$ | 106.0783 | - | - | - |
| Cumene | - | $C_9H_{12}$ | 120.0939 | - | - | - |

| | | | | | | |
|---|---|---|---|---|---|---|
| n-Propylbenzene | - | $C_9H_{12}$ | 120.0939 | - | - | - |
| n-Butylbenzene | - | $C_{10}H_{14}$ | 134.1096 | - | - | - |
| 3-Methyl-biphenyl | - | $C_{13}H_{12}$ | 168.0939 | - | - | - |
| 4-Methyl-biphenyl | - | $C_{13}H_{12}$ | 168.0939 | - | - | - |
| Sec-butylbenzene | - | $C_{10}H_{14}$ | 134.1096 | - | - | - |
| Styrene | - | $C_8H_8$ | 104.0626 | - | - | - |
| Toluene | - | $C_7H_8$ | 92.0626 | - | - | - |
| 2,4-dimethylstyrene | - | $C_{10}H_{12}$ | 132.0939 | - | - | - |
| 1,3-diisopropylbenzene | - | $C_{12}H_{18}$ | 162.1409 | - | - | - |
| Diphenylmethane | - | $C_{13}H_{12}$ | 168.0939 | - | - | - |
| Styrene-D8 | 13.46-13.58 | $C_8D_8$ | 112.1123 | -2.96 | 110.0982 | -3.45 |
| | | | | | 84.0841 | -3.81 |

Abbreviations: RTW=Retention time window

*Compounds without data "–" were not detected

**Table 3.** Biphasic kinetic model parameters and dissipation residual level ($RL_{50}$) of myclobutanil

| **Matrix** | **Tomato** | | **Grape** | |
|---|---|---|---|---|
| **Temperature** | **22°C** | **3°C** | **22°C** | **3°C** |
| **$C_0$ (µg/kg)** | 140.20 | 93.62 | 818.01 | 913.10 |
| **$k_1$ (hours$^{-1}$)** | 0.0025 | 0.0019 | 0.0027 | 0.0012 |
| **$k_2$ (hours$^{-1}$)** | 0.0027 | 0.0020 | 0.0029 | 0.0053 |
| **a** | 36.45 | 81.48 | 47.11 | 2.53 |
| **$RL_{50\ k1}$ (days)** | 11.52 | 15.28 | 10.59 | 24.02 |
| **$RL_{50\ k2}$ (days)** | 10.81 | 14.31 | 9.93 | 5.48 |
| **$R^2$** | 0.989 | 0.952 | 0.969 | 0.992 |

Abbreviations: $C_0$=Initial concentration; $k_1$ and $k_2$=Constant rates; a=Fraction of the initial chemical that degrades at the fast rate; $RL_{50}$=Residual level; $R^2$=Regression coefficient

**References**


(1) Botitsi, H.; Tsipi, D.; Economou, A. *Chapter 4. Current Legislation on Pesticides*; Elsevier, 2017. https://doi.org/10.1016/B978-0-12-809464-8.00004-X.

(2) Carrasco Cabrera, L.; Medina Pastor, P. The 2019 European Union Report on Pesticide Residues in Food. *EFSA Journal* **2021**, *19* (4), 1–89. https://doi.org/10.2903/j.efsa.2021.6491.

(3) Kotsonis, K. N.; Burdock, G. A. Chapter 31: Food Toxicology. In *Casarett & Doull's Essentials of Toxicology*; 2013; pp 1305–1356.

(4) Food and Agriculture Organization of the United Nations (FAO). FAOSTAT http://www.fao.org/faostat/es/#data/QCL (accessed 2021 -09 -15).

(5) Kashyap, A.; Silakari, O. Triazoles: Multidimensional 5-Membered Nucleus for Designing Multitargeting Agents. In *Key Heterocycle Cores for Designing Multitargeting Molecules*; Elsevier, 2018; pp 323–342. https://doi.org/10.1016/b978-0-08-102083-8.00009-1.

(6) University of Hertfordshire. PPDB: Pesticide Properties DataBase http://sitem.herts.ac.uk/aeru/ppdb/ (accessed 2021 -11 -30).

(7) Hao, W.; Hu, X.; Zhu, F.; Chang, J.; Li, J.; Li, W.; Wang, H.; Guo, B.; Li, J.; Xu, P.; Zhang, Y. Enantioselective Distribution, Degradation, and Metabolite Formation of Myclobutanil and Transcriptional Responses of Metabolic-Related Genes in Rats. *Environmental Science and Technology* **2018**, *52* (15), 8830–8837. https://doi.org/10.1021/acs.est.8b01721.

(8) Hergueta-Castillo, M. E.; López-Rodríguez, E.; López-Ruiz, R.; Romero-González, R.; Garrido Frenich, A. Targeted and Untargeted Analysis of Triazole Fungicides and Their Metabolites in Fruits and Vegetables by UHPLC-Orbitrap-MS2. *Food Chemistry* **2022**, *368*, 130860. https://doi.org/10.1016/j.foodchem.2021.130860.

(9) European Food Safety Authority. Conclusion on the Peer Review of the Pesticide Risk Assessment of the Active Substance Myclobutanil. *EFSA Journal* **2010**, *8* (10), 1–83. https://doi.org/10.2903/j.efsa.2010.1783.

(10) European Commission. Regulation (EC) No 1107/2009. *Official Journal of the European Union* **2009**, *24* (8), 1–50.

(11) Markets and Markets, Agricultural Adjuvants Market by Function (Activator and Utility), Application (Herbicides, Insecticides, and Fungicides), Formulation (Suspension Concentrates and Emulsifiable Concentrates), Adoption Stage, Crop Type, and Region. Global Forecast 2026 https://www.marketsandmarkets.com/Market-Reports/adjuvant-market-1240.html (accessed 2022 -02 -02).

(12) Maldonado-Reina, A. J.; López-Ruiz, R.; Garrido Frenich, A.; Arrebola, F. J.; Romero-González, R. Co-Formulants in Plant Protection Products: An Analytical Approach to Their Determination by Gas Chromatography–High Resolution Mass Accuracy Spectrometry. *Talanta* **2021**, *234*, 122641. https://doi.org/10.1016/j.talanta.2021.122641.

(13) Balmer, M. E.; Janser, D.; Schaller, U.; Krauss, J.; Geiser, H. C.; Poiger, T. Magnitude and Decline of Pesticide Co-Formulant Residues in Vegetables and Fruits: Results from Field Trials Compared to Estimated Values. *Pest Management Science* **2021**, *77* (3), 1187–1196. https://doi.org/10.1002/ps.6128.

(14) European Commission. COMMISSION REGULATION (EU) 2021/383. *Official Journal of the European Union* **2021**, *L74*, 7–26.

(15) The European Commission. EU pesticides database https://ec.europa.eu/food/plant/pesticides/eu-pesticides-database/active-substances/?event=search.as.

(16) Liu, Y.; Sun, H.; Liu, F.; Wang, S. Dissipation and Residue of Myclobutanil in Lychee. *Bulletin of Environmental Contamination and Toxicology* **2012**, *88* (6), 902–905. https://doi.org/10.1007/s00128-012-0610-2.

(17) Michel, A.; Brauch, H.-J.; Worch, E.; Lange, F. T. Development of a Liquid Chromatography Tandem Mass Spectrometry Method for Trace Analysis of Trisiloxane Surfactants in the Aqueous Environment: An Alternative Strategy for Quantification of Ethoxylated Surfactants. *Journal of Chromatography A* **2012**, *1245*, 46–54. https://doi.org/10.1016/j.chroma.2012.04.064.

(18) Oliver-Rodríguez, B.; Zafra-Gómez, A.; Camino-Sánchez, F. J.; Conde-González, J. E.; Pérez-Trujillo, J. P.; Vílchez, J. L. Multi-Residue Method for the Analysis of Commonly Used Commercial Surfactants, Homologues and Ethoxymers, in Marine Sediments by Liquid Chromatography-Electrospray Mass Spectrometry. *Microchemical Journal* **2013**, *110*, 158–168. https://doi.org/10.1016/j.microc.2013.03.006.

(19) Lara-Martín, P. A.; González-Mazo, E.; Brownawell, B. J. Multi-Residue Method for the Analysis of Synthetic Surfactants and Their Degradation Metabolites in Aquatic Systems by Liquid Chromatography-Time-of-Flight-Mass Spectrometry. *Journal of Chromatography A* **2011**, *1218* (30), 4799–4807. https://doi.org/10.1016/j.chroma.2011.02.031.

(20) Cao, L.; Jiang, H.; Yang, J.; Fan, L.; Li, F.; Huang, Q. Simultaneous Determination of Benzene and Toluene in Pesticide Emulsifiable Concentrate by Headspace GC-MS. *Journal of Analytical Methods in Chemistry* **2013**, *2013*, 1–5. https://doi.org/10.1155/2013/121783.

(21) Prata, R.; López-Ruiz, R.; Henrique Petrarca, M.; Teixeira Godoy, H.; Garrido Frenich, A.; Romero-González, R. Targeted and Non-Targeted Analysis of Pesticides and Mycotoxins in Baby Foods ByUHPLC-Q-Orbitrap-MS. *submitted*.

(22) Pihlström, T.; Fernández-Alba, A. R.; Ferrer Amate, C.; Erecius Poulsen, M.; Lippold, R.; Carrasco Cabrera, L.; Pelosi, P.; Valverde, A.; Mol, H.; Jezussek, M.; Malato, O.; Štěpán, R. Analytical Quality Control and Method Validation Procedures for Pesticide Residues Analysis in Food and Feed SANTE 11312/2021. **2021**, 1–57.

(23) Marín-Sáez, J.; Romero-González, R.; Garrido Frenich, A. Multi-Analysis Determination of Tropane Alkaloids in Cereals and Solanaceaes Seeds by Liquid Chromatography Coupled to Single Stage Exactive-Orbitrap. *Journal of Chromatography A* **2017**, *1518*, 46–58. https://doi.org/10.1016/j.chroma.2017.08.052.

(24) López-Ruiz, R.; Romero-González, R.; Ortega-Carrasco, E.; Garrido Frenich, A. Dissipation Studies of Famoxadone in Vegetables under Greenhouse Conditions Using Liquid Chromatography Coupled to High-Resolution Mass Spectrometry: Putative Elucidation of a New Metabolite. *Journal of the Science of Food and Agriculture* **2019**, *99* (12), 5368–5376. https://doi.org/10.1002/jsfa.9794.

(25) Fantke, P.; Juraske, R. Variability of Pesticide Dissipation Half-Lives in Plants. *Environmental Science and Technology* **2013**, *47* (8), 3548–3562. https://doi.org/10.1021/es303525x.

(26) Whitmyre, G. K.; Ross, J. H.; Lunchick, C.; Volger, B.; Singer, S. Biphasic Dissipation Kinetics for Dislodgeable Foliar Residues in Estimating Postapplication Occupational Exposures to Endosulfan. *Archives of Environmental Contamination and Toxicology* **2004**, *46* (1), 17–23. https://doi.org/10.1007/s00244-003-2166-y.

(27) López-Ruiz, R.; Romero-González, R.; Garrido Frenich, A. Residues and Dissipation Kinetics of Famoxadone and Its Metabolites in Environmental Water and Soil Samples under Different Conditions. *Environmental Pollution* **2019**, *252*, 163–170. https://doi.org/10.1016/j.envpol.2019.05.123.

(28) Sun, C.; Cang, T.; Wang, Z.; Wang, X.; Yu, R.; Wang, Q.; Zhao, X. Degradation of Three Fungicides Following Application on Strawberry and a Risk Assessment of Their Toxicity under Greenhouse Conditions. *Environmental Monitoring and Assessment* **2015**, *187* (5). https://doi.org/10.1007/s10661-015-4539-x.

(29) Salunkhe, V. P.; Sawant, I. S.; Banerjee, K.; Wadkar, P. N.; Sawant, S. D. Enhanced Dissipation of Triazole and Multiclass Pesticide Residues on Grapes after Foliar Application of Grapevine-Associated Bacillus Species. *Journal of Agricultural and Food Chemistry* **2015**, *63* (50), 10736–10746. https://doi.org/10.1021/acs.jafc.5b03429.

(30) Hlihor, R. M.; Pogăcean, M. O.; Rosca, M.; Cozma, P.; Gavrilescu, M. Modelling the Behavior of Pesticide Residues in Tomatoes and Their Associated Long-Term Exposure Risks. *Journal of Environmental Management* **2019**, *233*, 523–529. https://doi.org/10.1016/j.jenvman.2018.11.045.

(31) Ontario Ministry of the Environment (MOE). *Ontario Air Standards for Trimethylbenzenes: 1,2,3-Trimethylbenzene 1,2,4-Trimethylbenzene 1,3,5-Trimethylbenzene*; 2007.

Table of content